Multidimension potential of surface plasmon resonance imaging for dynamic surface characterization: Application to optical biochips

P. Lecaruyer[1], E. Maillart[1], M. Canva[1] and J. Rolland[1,2]
[1]*Laboratoire Charles Fabry de l'Institut d'Optique, Université Paris-Sud d'Orsay, bât.503 Centre Scientifique, 91403 Orsay cedex,France*
pierre.lecaruyer@iota.u-psud.fr
[2]*Permanent adress: College of Optics and Photonics: CREOL&FPCE, University of Central Florida, Orlando FL 32816-2700, USA*
jannick@odalab.ucf.edu

ABSTRACT

We have realized a surface plasmon resonance imaging system allowing accurate characterization of biochips. In this paper, the Rouard approach is extended to absorbing layers to model the reflectivity information contained in the multidimensional data. The multidimension potential is also expressed to demonstrate the power of the SPR imaging system. To conclude, towards the development of a biosensor based on SPR, a theoretical study is also performed on the sensitivity to changes in reflectivity of such multidimension optical biosensor. The sensitivity of the sytem shows the power of this biophotonic technology.

Keywords: surface plasmon resonance, Rouard, multidimension, biochips.

1. EXTENDED ROUARD METHOD FOR MODELLING REFLECTIVITY OF MULTIPLE LAYERS THIN FILMS

The conventional approach to determining the amplitudes and intensities of beams of light reflected off a thin film of multiple layers consists in setting up Maxwell's equations together with the appropriate boundary conditions. Such approach is conventionally implemented using a matrix formulation, such as first provided by Abeles [1] and further developped by Yeh [2].

Another approach to the problem is what we shall refer to as the extended Rouard approach. The beauty of the method lies in its simple implementation and generalization to as many layers as needed, with no added complexity [3]. Furthermore, we shall yield new insight into the Snell's law of refraction when operating beyond the equivalent critical angle between the entry and the exit layer. The approach emerges from the consideration that a single film bounded by two surfaces possesses an effective reflection coefficient and accompanying phase change. Thus, a thin film may be replaced by a single equivalent surface with such properties. However, Rouard limited his treatment to transparent layers. Although Heavens [4] provided a different method for absorbing layers, it yield extremely convoluted expressions. In fact with a proper handling of the terms that make the Snell's law invariant, we shall now provide an extension to the Rouard method generally applicable to any multiple layers thin films, including those with any number of absorbing layers.

Let us consider Fig.1. In this figure, multiple thin film and substrate layers are stacked together. In the context of our experimental setup of plasmon resonance surface, the layers going from the bottom to the top correspond to the coupling prism, a glass plate acting as a substrate for the thin film deposition, a chromium thin film, a gold thin film, and the cover medium made of an aqueous buffer solution, where the molecular interactions occur between the molecules within the solution and the molecules pre-attached to the gold layer. From the electromagnetic theory and the setting of Maxwell's equations together with proper continuity boundary conditions, the resulting invariant Snell's law of refraction when applied to the stack of layers shown takes the form

$$n_1 \sin\theta_1 = n_2 \sin\theta_2 = n_3 \sin\theta_3 = n_4 \sin\theta_4 = n_5 \sin\theta_5 \quad , \qquad (1)$$

Diagnostic Optical Spectroscopy in Biomedicine III, edited by Mary-Ann Mycek,
Proc. of SPIE-OSA Biomedical Optics, SPIE Vol. 5862, 58620H, © 2005 SPIE-OSA · 1605-7422/05/$15

where, if any medium is absorbing, the corresponding index of refraction takes the form of a complex term. Replacing n_2 with $n_2=a_{n2}+i\ b_{n2}$ (a and b being real values), for example, we can write

$$sin\theta_2 = n_0 sin\theta_0 / (a_{n2}+i\ b_{n2}) \quad . \tag{2}$$

The prism being made of glass, we can deduce that $sin\theta_2$ is complex. Thus a fundamental observation to this framework is to realize that for an absorbing medium, not only the index of refraction takes on a complex form, but the associated $sin\theta$ is also complex. Thus, the geometrical optic notion of θ as an angle is naturally lost under such light propagation condition. If we now consider the phase change for the light going through the i^{th} layer we have

$$\varphi = \frac{2\pi}{\lambda} n_i e_i \cos\theta_i \quad , \tag{3}$$

where λ is the wavelength, n_i is the index of refraction, e_i is the physical thickness of the layer, and θ_i is the associated term of the Snell's invariant. From the expression provided by Eq. 3, the product $n_i \cos(\theta_i)$ will be of complex form, a ± ib, as will $\cos(\theta_i) = \sqrt{1-\sin^2(\theta_i)}$. In the case of an electromagnetic field of the form $e^{i\varphi}$, the positive sign corresponds to an absorbing medium. Thus one cannot simply insert the index of refraction n to be of the form $a_n + ib_n$, instead one must set the Snell's law invariant of the proper form.

To apply the Rouard method to a stack of non-necessarily transparent layers, we shall capitalize on the expression of reflectivity for a single thin film located between two layers. Without loss of generality, let's consider the gold layer of index of refraction n_4, thickness e_4, and Fresnel coefficient of reflection $r_{4\text{-}5}$. Layer 4 lies between layer 5 of index of refraction n_5 and layer 3 of index of refraction n_3, thickness e_3 , and Fresnel coefficient of reflection $r_{3\text{-}4}$.

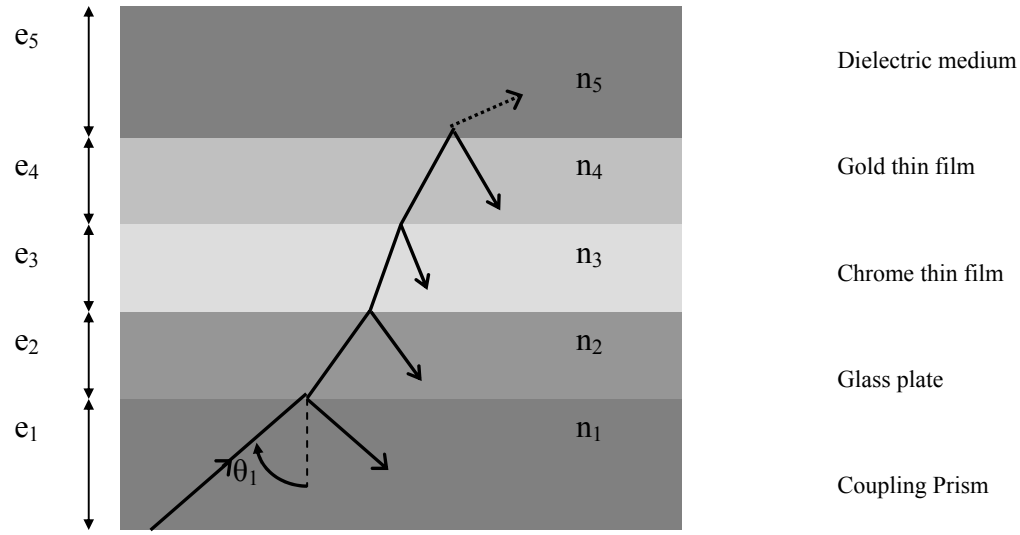

Fig.1. Stack of multiple thin films and substrates of various thicknesses and refractive indexes, where any layer could be an absorbing media.

It can be shown that the effective Fresnel coefficient for layer 3 is provided by the expression [3]

$$R_4 = \frac{r_{3-4} + r_{4-5} e^{2i\varphi_4}}{1 + r_{3-4} r_{4-5} e^{2i\varphi_4}} \quad , \tag{4}$$

which is complex. Eq. (4) is derived by summing up the multiple reflected and transmitted beams off the layer and using the principle of conservation of energy. We can now consider the system from layer 3 to layer 1 as a stack lying on an

equivalent surface of Fresnel coefficient R_4 . The effective Fresnel coefficient of reflection for the equivalent layer 3 and above is then given by

$$R_3 = \frac{r_{2-3} + R_4 e^{2i\varphi_3}}{1 + r_{2-3} R_4 e^{2i\varphi_3}} \quad . \tag{5}$$

Equivalently, R_2 and R_1 may be expressed by recursion applying the equivalent expression used to derive Eq (4-5). This expression is general and applies to any angle of incidence, wavelength, and polarization with the proper Fresnel coefficients. Across multiple wavelengths, the reflectivity coefficients sum up.

2. MULTIDIMENSION SURFACE PLASMON RESONANCE

We have realized a multidimensional imaging sensor that demonstrates the impact of all the surface plasmon resonance physical parameters on the quality of the measurement and that demonstrates the potential of this sensor to biochip systems. The more we learn about the surface under investigation (2D spatial dimension) from numerous ways of characterization, the higher the probability of extracting information on its physical characteristics. All the dimensions of the system data can be divided into two groups. First, the three dimensions linked to the illuminating beam, which are the angle of incidence on the surface, the wavelength, and the state of polarization. (i.e. TM_x and TM_y). Next, the multidimensional SPR imaging system is a real-time sensor, adding the temporal dimension.

2.1. Angle of incidence, wavelength and polarization.

The angle of incidence and the wavelength have a similar effect on the shape of the plasmon curve. This is illustrated in Fig.2 in which the reflectivity in TM mode is plotted as a function of the angle of incidence on the surface and as a function of wavelength.

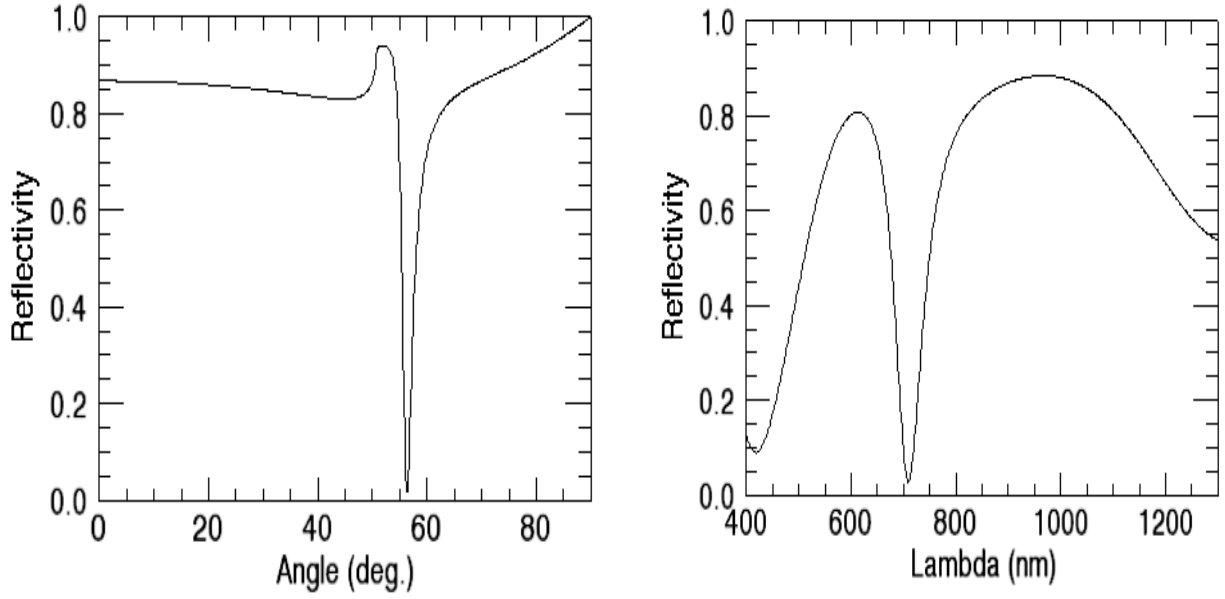

(a) (b)

Fig. 2. (a) Reflectivity in TM mode as a function of the incident angle and (b) wavelength for a SF11-gold-water configuration.

However, the former only changes the coupling efficiency (Eq.6) while the latter changes both the coupling efficiency and the plasmon resonance condition (i.e. the plasmon **k** vector, Eq. 7):

$$k_{\mathrm{P}} = \frac{2\pi}{\lambda} n_{prism} \sin\theta \,, \tag{6}$$

$$k_{plasmon} = \mathrm{Re}\left(\sqrt{\frac{\varepsilon_m \varepsilon_d}{\varepsilon_m + \varepsilon_d}} \right) \frac{w}{c} \,, \tag{7}$$

where ε_m and ε_d represent the permittivity respectively of the metallic layer and the dielectric medium. Moreover, the effective index of the plasmon is modified by the dispersion of the materials involved in the reflectivity modelling and illustrated in Fig. 3.

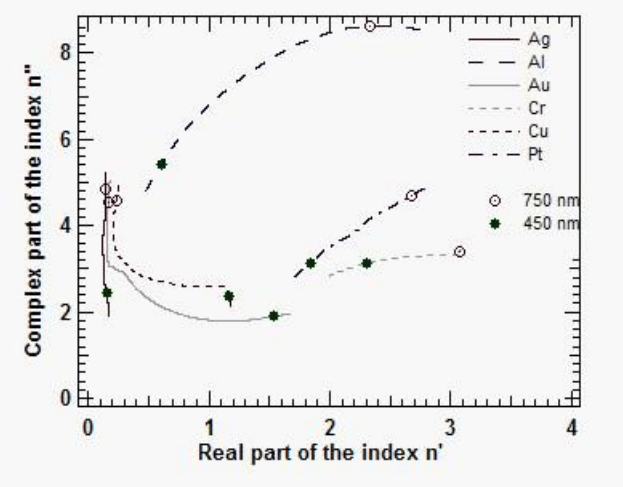

Fig. 3. Trajectories of the refractive index of various metals as a function of the wavelength illustrating the dispersion of metals in the visible range.

This link between the two dimensions is illustrated in Fig.4 in which the reflectivity is plotted as a function of the two dimensions. Therefore both parameters play a key role in monitoring the surface chemistry.

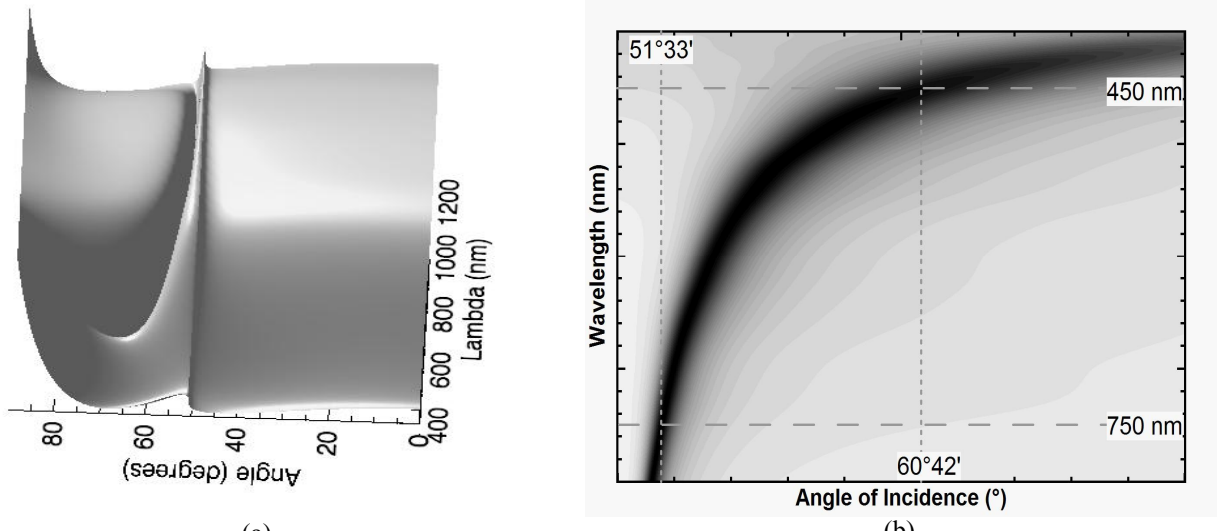

(a) (b)

Fig. 4. (a) 3D- reflectivity in TM mode as a function of the incident angle on the surface and the wavelength for a SF11-gold-water configuration.(b) Map of reflectivity as a function of the incident angle and the wavelength for a SF11-silver-water configuration.

Furthermore, and importantly, the SPR system is also a polarimetric sensor. In application to biosensors, because the molecules could land on the surface with a particular orientation due to the fluidics in the interaction cell, it could allow to measure anisotropy of the deposited layer by adapting the imaging system, using two orthogonal beams. This is a way to measure noise dispersion as a function of the fluidics parameters such as the speed of the aqueous flux or the cell geometry.

2.2. Time and spatial dimensions.

The SPR sensor is also a real-time imaging system. This particularity allows the measurement of the dynamic evolution of the layer at each pixel of the image. In application to optical biochips, knowing the kind of interactions between the functionalized surface and the molecules and the impact of this interaction on the reflectivity shape, we can analyse and monitor in real-time the kinetics of the interaction. Measuring the molecular density deposition on the surface is important but actually measuring chemical constants yields much more possibilities (i.e. association and dissociation rates) at each step of the kinetics [5] as illustrated in fig.5. In this figure, the dynamics of interactions show different slopes that illustrate different speeds of interaction between different probes and the same target.

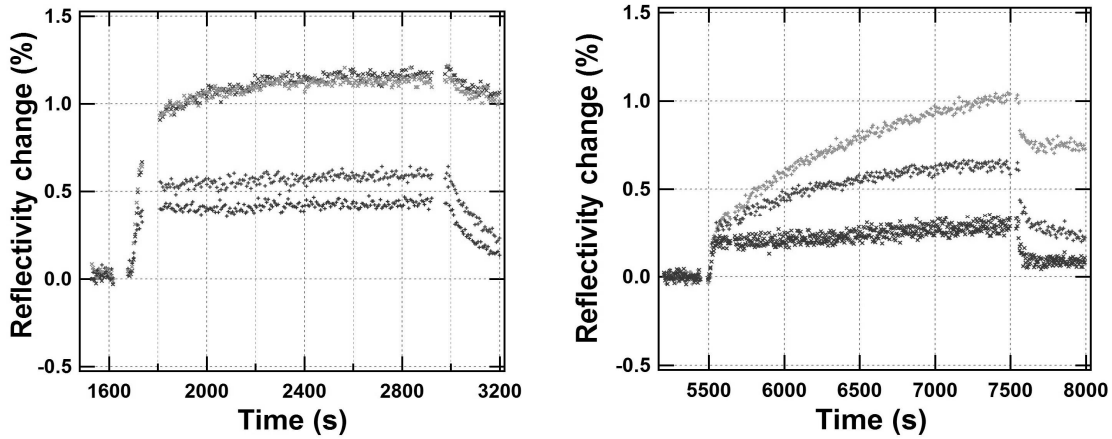

Fig. 5. (left) Dynamics of interactions between a functionalized surface and DNA molecules. The signal remaining after rinsing 3000s is proportional to the matter quantity deposited.(right) Dynamics of interactions between a functionalized surface and DNA molecules. After extraction of association and dissociation rates, it illustrates the difference of speed of biomolecular interaction

Moreover, the imaging system allows to analyse up to 200 parallel interactions while actual commercial SPR systems only allow up to 4 parallel analyses [6,7] as illustrated in fig.6.

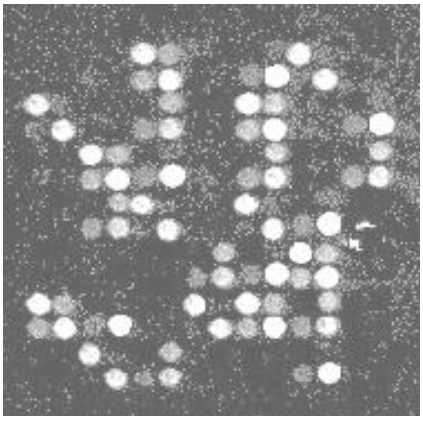

Fig. 6. Image recorded after the rinsing of the interaction between a functionalized surface (for cystic fibrosis mutation diagnostic) and DNA oligonucleotides. This picture illustrates the high specificity of reponse of the surface. The areas in black represent the surface where no molecules interact at all.

It is then possible to compare the kinetics in real-time through the surface by changing a parameter like the density of molecules grafted on the surface or the mutation of a DNA-sequence. The precision of the measurements depends on the use of each of the 6 dimensions that allows many means of calibration of the optical signal.

3. SENSITIVITY AND PRECISION OF THE SURFACE CHARACTERIZATION

The SPR technique is based on the sensing of the properties of an evanescent field generated at the site of total internal reflection on a metallic surface. SPR is a charge density oscillation that may exist at the interface of two media with dielectric constants of opposite signs, i.e. a dielectric (e.g. aqueous solution) and a metal (e.g. gold). The charge density wave is associated with an optical evanescent wave localized on each side of the interface. These evanescent waves can be highly asymmetric. Under our approach to SPR, one wave typically penetrates the metal layer a few nanometers, while the other penetrates the dielectric medium a few tens of nanometers. We have shown that small refractive index changes of the adjacent medium to the gold surface modifies the propagation of the evanescent wave and creates a shift in the reflectivity curve as a function of the dependent variable [6,7] As previously mentioned, the experiments and calculations using either the angular or spectral dependence of the light beam have the same effect on the shape of the plasmon curve. However, it is interesting to study the influence of the dispersion of these two parameters on the sensitivity and precision of the method of measurement because in our methodology we do not measure a minimum shift in the reflectivity curve in TM mode but a variation in reflectivity at the point of highest slope on that curve given a biological layer. Such typical curves were shown in Fig. 2a or 2b.

The high sensitivity of the method is caused by the plasmon resonant dependence on the parameters (i.e. amplitude and phase) of the light beam reflected off the metal surface, but also by the choice of the point of highest slope as the point of measure. Also, the theoretical reflectivity as a function of the biological layer thickness occurring through binding to the metallic layer shown in Fig.7 displays a quasi-linear zone of high slope.

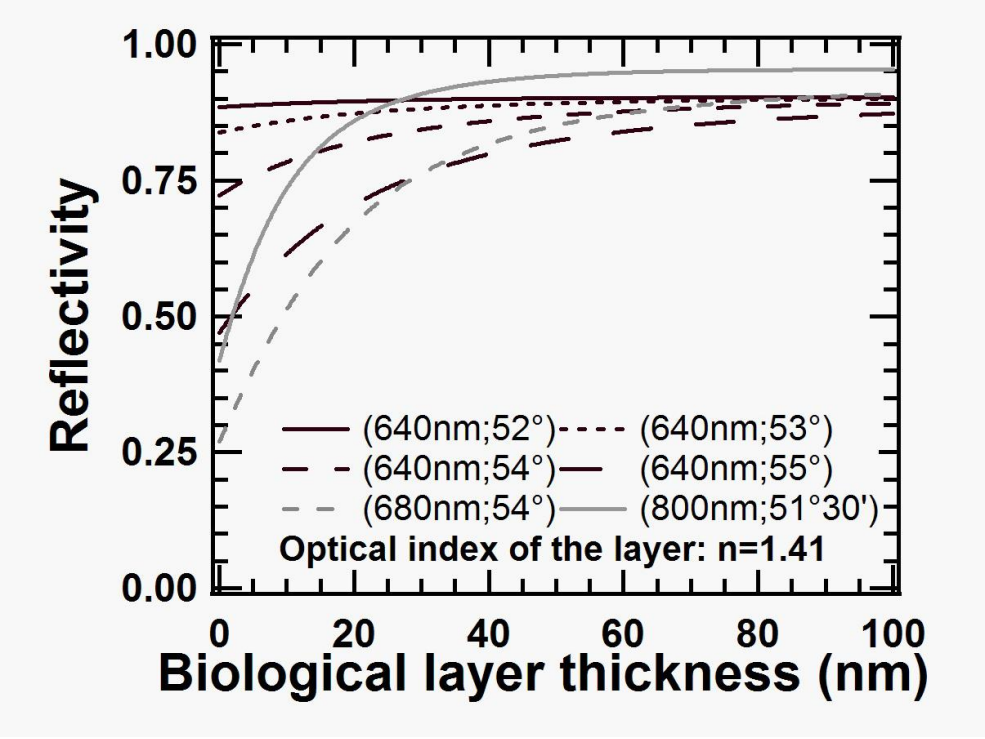

Fig. 7. Example of theoretical reflectivity variations due to the growth of a biological layer of refractive index n= 1.41 in water for different couple of wavelengths and angles of incidence.

As a result, this allows a high sensitivity of a few percent per nanometer in this region for small layer thickness depositions for various beam characteristics (i.e. wavelength and angle of incidence) as illustrated in fig.8.

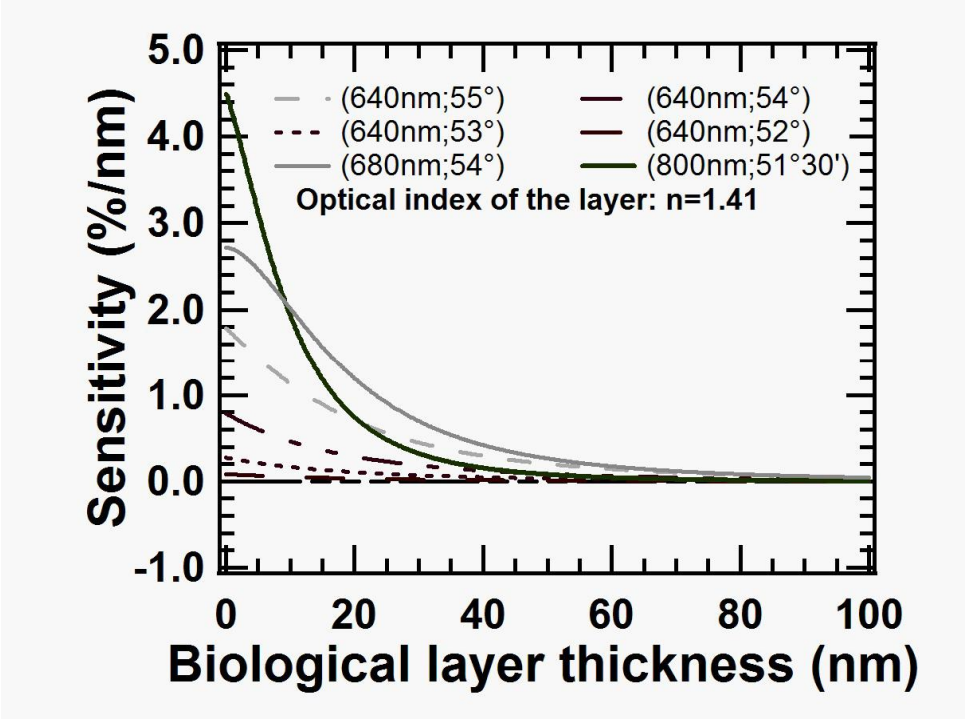

Fig. 8. Example of theoretical sensitivity as a function of a biological layer of refractive index n= 1.41 in water for different couple of wavelengths and angles of incidence. The sensitivity was obtained by derivation of the reflectivity curves of fig.7.

Experimentally with a non-ideal light source (i.e. slight variation in the angle of incidence and quasi-monochromatic light source), the resulting plasmon curve corresponds to an integration of the various responses to each angle of incidence and wavelength, but the linearity of the response allows maintaining high sensitivity. As a result, for example, a 4 mrad angular dispersion and a spectral dispersion of 20 nm on a 660 nm illuminating source yields a loss in SPR sensitivity of less than 5% [8].

Another trade-off related to sensitivity is that of resolution. Increasing the wavelength to IR allows increasing the sensitivity of the optical sensor as a consequence of an increase in the SPR propagation length. Naturally, such increase results in less resolution. Next, the influence of the wavelength on the homogeneity, and thus the precision, of the response is primordial and is under investigation.

Finally, it is important to emphasize that the imaging system captures a two dimensional picture of the 2D biochip in real-time. The precision of the biological measurement is directly linked to the number of measures performed in the 6D space. However, the imaging also allows through a simple calibration procedure characterization of the homogeneity of the layer stack throughout the entire surface at each pixel. This measure provides a dispersion measurement which can be employed in further optimizing precision. Also, a factor of quality of the layer stack deposition can be extracted.

4. CONCLUSION

The Rouard method has been extended to as many absorbing layers as needed and was implemented to numerical calculations of multilayer stack including metal-dielectric interface allowing plasmon resonance. This allowed to model reflectivity as a function of all the dimensions involved in a biochip and was applied to configure the optical system used to analyse interactions on biochips. The configuration of the system allows calibration of the optical signal by different means of measurement. Ongoing experiments validating the potential of such multidimensional data approach for robust and accurate surface characterization are being performed in connection with dynamic biochip systems applied to genomics and proteomics.

Investigations on the dispersion of materials are also investigated in the aim of extending the system to UV or IR range in which the dispersion could have a primordial influence on sensitivity.

5. REFERENCES

1. F. Abelès, *Ann. Physique* **5**, 596, 706 (1950).
2. P. Yeh, "Optical Waves in Layered Media", *Wiley & Sons*, 1988, X-pp. 406.
3. P. Rouard, *Ann. Physique* **11**, 342 (1950).
4. O.S. Heavens, *Optical properties of thin solid films* (Dovers Publications, Inc. NY, 1965) p65.
5. E. Maillart, K.Brengel-Pesce et al., "Versatile analysis of macromolecular interactions by SPR imaging : application to p53 and DNA interaction", Oncogene, **23**, 5543-5550 (2004).
6. www.biacore.com/technology/core.lasso
7. N. Bassil, E.Maillart *et al.*, "One hundred spots parallel monitoring of DNA interactions by SPR imaging of polymer-functionalized surfaces applied to the detection of cystic fibrosis mutations", Sens. Actuators B, **94**, 313-323 (2003).
8. E. Maillart, *Développement d'un système optique d'imagerie en résonance de plasmon de surface pour l'analyse simultanée de multiples interactions biomoléculaires en temps réel* (PhD thesis speciality : Optics, Université Paris XI, 2004), Chap.2.